

## STRUCTURE NOTE

# Crystal structure of LZ-8 from the medicinal fungus *Ganoderma lucidum*

Liang Huang,<sup>1</sup> Fei Sun,<sup>2</sup> Chongyang Liang,<sup>2</sup> Yong-Xing He,<sup>1</sup> Rui Bao,<sup>1</sup> Lixia Liu,<sup>3\*</sup> and Cong-Zhao Zhou<sup>1\*</sup>

<sup>1</sup> Hefei National Laboratory for Physical Sciences at Microscale, School of Life Sciences, University of Science and Technology of China, Hefei, Anhui 230027, People's Republic of China

<sup>2</sup> Department of Cytobiology, Institute of Frontier Medical Science, Jilin University, Changchun 130021, People's Republic of China

<sup>3</sup> School of Life Sciences, Northeast Normal University, Changchun 130024, People's Republic of China

**Key words:** fungal immunomodulatory proteins; *Ganoderma lucidum*; crystal structure; antitumor activity.

## INTRODUCTION

Ling Zhi (*Ganoderma lucidum*) and other medicinal fungi have a long history of use as traditional herbs in China. The mechanism of their effects for a wide range of ailments remains unclear. To elucidate the functional compounds in these herbs, a new family of fungal immunomodulatory proteins (Fips) has been identified, including four Fips isolated from *Ganoderma lucidum*, *Flammulina velutipes*, *Volvariella volvacea*, and *Ganoderma tsugae*, termed LZ-8, Fip-gts, Fip-fve, and Fip-vvo, respectively.<sup>1–4</sup>

The native LZ-8 has a series of biological activities which include immunomodulatory responses,<sup>3</sup> alleviation of transplant rejection,<sup>4</sup> and antitumor activity. In terms of antitumor activity, LZ-8 plays a role as a mitogen in mouse spleen cells,<sup>5</sup> human peripheral lymphocytes,<sup>6</sup> and peripheral mononuclear cells.<sup>4</sup> Fip-gts from *G. tsugae*, which shares an identical primary sequence to LZ-8, was found to perform its antitumor activity by triggering calcium signaling in repression of telomerase activity and inhibiting the transcription of telomerase in human lung adenocarcinoma cell line A549, via exporting the telomerase reverse transcriptase out of the nuclei.<sup>7,8</sup>

Despite being highly conserved in primary sequence, members of Fips family are quite different from each other in biological activity.<sup>9</sup> For instance, LZ-8 has a strong antitumor activity against HL60 cells, whereas Fip-fve has no such an activity (unpublished data), even though they share a sequence similarity of 81%. To eluci-

date the structural basis of this functional divergence, we solved the crystal structure of LZ-8 at 2.10 Å resolution (PDB code 3F3H), representing the second structure in this family after Fip-fve.<sup>10</sup> Comparative structural analyses revealed significant local conformation changes at two loop regions of the fibronectin type III (FNIII) domain which might be potential active sites. This finding provided us clues for engineering these loops to further improve the medicine activity of LZ-8 and its homologs.

## MATERIALS AND METHODS

### Construction, expression, and purification of LZ-8

The open reading frame of LZ-8 was amplified by PCR and cloned into a p819 expression vector. The con-

Liang Huang and Fei Sun contributed equally to this work.

Grant sponsor: Ministry of Science and Technology of China; Grant numbers: 2006CB910202, 2006CB806501; Grant sponsor: Chinese National Natural Science Foundation; Grant number: 30870490; Grant sponsors: Chinese Academy of Science (100-Talent Project), USTC.

\*Correspondence to: Lixia Liu, School of Life Sciences, Northeast Normal University, Changchun 130024, People's Republic of China. E-mail: liulx062@nenu.edu.cn; or Cong-Zhao Zhou, Hefei National Laboratory for Physical Sciences at Microscale, School of Life Sciences, University of Science and Technology of China, Hefei, Anhui 230027, People's Republic of China. E-mail: zcz@ustc.edu.cn  
Received 7 November 2008; Accepted 25 November 2008

Published online 11 December 2008 in Wiley InterScience (www.interscience.wiley.com). DOI: 10.1002/prot.22346

struct was transferred to *Pichia pastoris* GS115. The transfected cells were grown in MD and MM medium for determination of methanol-utilizing phenotype at 28°C up to an  $A_{600\text{ nm}}$  of 2–6. The protein expression was induced by adding methanol to a final concentration of 1% in the medium and the cells were grown at 28°C for 72 hr. Cell pellet and supernatant were separated and frozen in liquid nitrogen and stored at –70°C for next purification. Approximately 50 mL supernatant was thawed and loaded to the Q Sepharose HP 35/100 column followed by Hiload 16/60 Superdex 75 column (Amersham Biosciences). The purity of the pooled fractions was checked by SDS-PAGE. The protein sample was concentrated to 8 mg/mL in the buffer of 50 mM NaCl, 20 mM Tris-HCl, pH 7.0 for further use.

### Crystallization, data collection, and processing

The crystal was grown at 289 K using the hanging drop vapor diffusion method. Two microliters of the protein solution was mixed with 1  $\mu\text{L}$  of mother liquor (1.75M ammonium sulfate, 0.1M Tris-HCl, pH 6.0 and 6.4% polyethylene glycol 400). The rhombic crystals grew to the maximal size of  $110 \times 100 \times 30 \mu\text{m}^3$  in one week. A single crystal was transferred to the cryoprotectant buffer of the reservoir solution plus 20% polyethylene glycol 400 and flash frozen with liquid nitrogen. X-ray diffraction data were collected at 100 K on a Rigaku MM007 X-ray generator ( $\lambda = 1.54179 \text{ \AA}$ ) with a MarResearch 345 image-plate detector at School of Life Sciences, University of Science and Technology of China (USTC, Hefei, PR China). Data were processed with the Program MOSFLM<sup>11</sup> and scaled with SCALA.<sup>12</sup>

### Structure solution and refinement

The crystal belongs to the space group of  $P2_12_12_1$  with a homodimer in an asymmetric unit. The crystal structure of LZ-8 was solved by the molecular replacement method with the program Molrep<sup>12</sup> of CCP4 using the fungal immunomodulatory protein Fip-fve (PDB entry 1OSY) as the search model. Crystallographic refinement was performed using the program Refmac5.<sup>12</sup> After several rounds of manual rebuilding and water picking using the graphics program COOT,<sup>13</sup> TLS parameters were analyzed with the TLSMD server<sup>14</sup> and four TLS groups for each chain were introduced in the subsequent refinement. The stereochemical quality of the final model was validated with Molprobit<sup>15</sup> and PROCHECK.<sup>16</sup> The structure was finally refined to 2.10  $\text{Å}$  with the R-factor 22.1% and R-free 24.6%, respectively. The structure factor and coordinate files were deposited in the Protein Data Bank under the accession code of 3F3H. All figures of protein structure were prepared with PyMol.<sup>17</sup>

**Table I**

Crystal Parameters, Data Collection, and Structure Refinement

Data processing	
Space group	$P2_12_12_1$
Unit cell parameters a, b, c ( $\text{Å}$ )	33.19, 86.99, 92.13
$\alpha, \beta, \gamma$ ( $^\circ$ )	90, 90, 90
Resolution range ( $\text{Å}$ )	22.89–2.10 (2.21–2.10) <sup>a</sup>
Unique reflections	15,951 (2167)
Completeness (%)	98.0 (93.6)
$\langle I/\sigma(I) \rangle$	11.1 (4.1)
$R_{\text{merge}}^b$ (%)	12.5 (30.2)
Redundancy	4.8
Refinement statistics	
Resolution range ( $\text{Å}$ )	20.00–2.10
R-factor <sup>c</sup> /R-free <sup>d</sup> (%)	22.1/24.6
Number of protein atoms	1752
Number of water atoms	74
RMSD <sup>e</sup> bond length ( $\text{Å}$ )	0.008
RMSD bond angles ( $^\circ$ )	1.054
Average of B factors ( $\text{Å}^2$ )	13.5
Ramachandran plot <sup>f</sup>	
Most favored (%)	98.14
Additional allowed (%)	1.86
Outliers (%)	0
PDB entry	3F3H

<sup>a</sup>The values in parentheses refer to statistics in the highest bin.

<sup>b</sup> $R_{\text{merge}} = \sum_{\text{hkl}} \sum_i |I_i(\text{hkl}) - \langle I(\text{hkl}) \rangle| / \sum_{\text{hkl}} \sum_i I_i(\text{hkl})$ , where  $I_i(\text{hkl})$  is the intensity of an observation and  $\langle I(\text{hkl}) \rangle$  is the mean value for its unique reflection; Summations are over all reflections.

<sup>c</sup>R-factor =  $\sum_h |F_o(h) - F_c(h)| / \sum_h F_o(h)$ , where  $F_o$  and  $F_c$  are the observed and calculated structure-factor amplitudes, respectively.

<sup>d</sup>R-free was calculated with 5% of the data excluded from the refinement.

<sup>e</sup>Root-mean square-deviation from ideal values.

<sup>f</sup>Categories were defined by Molprobit.

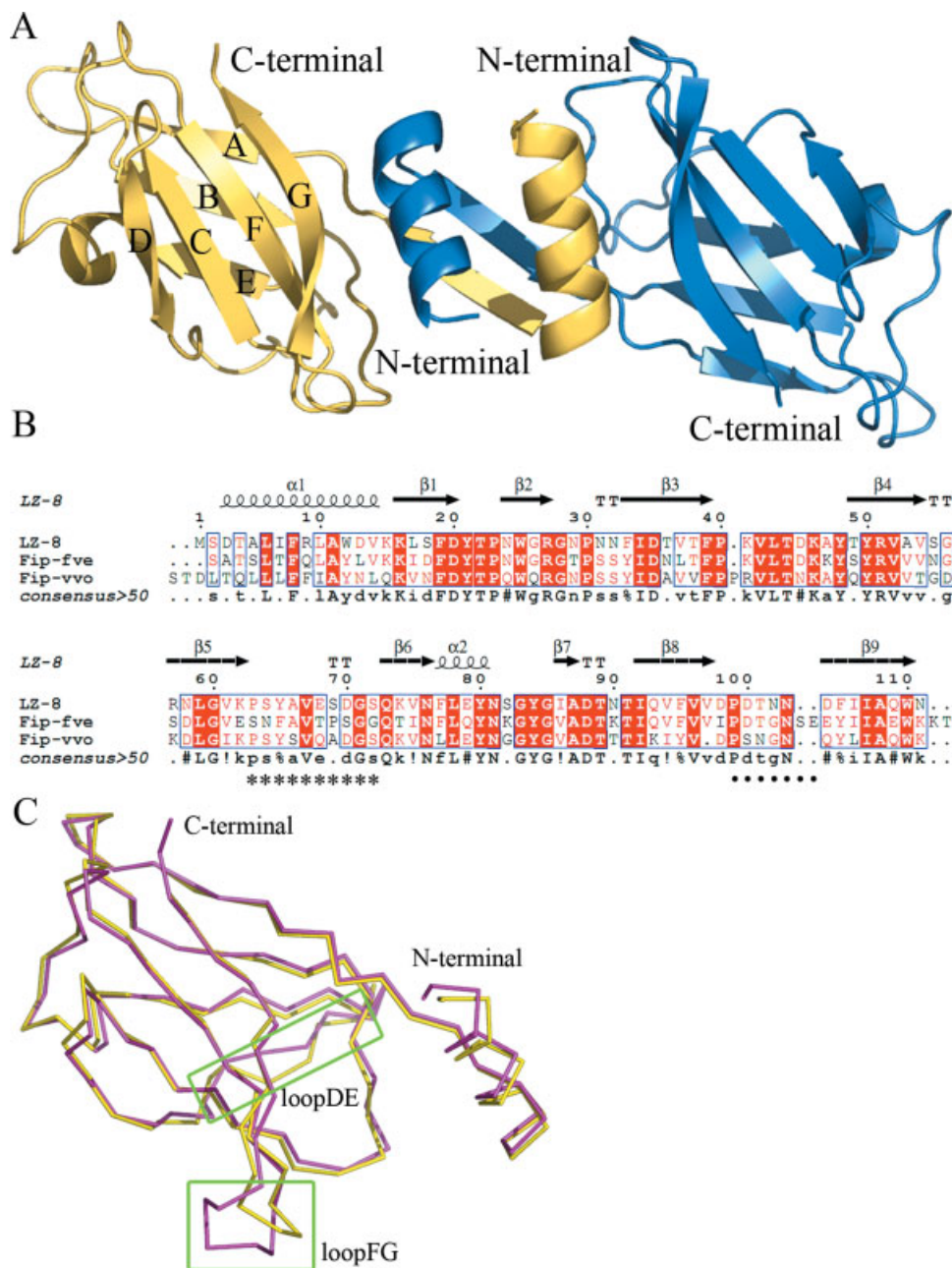
## RESULTS AND DISCUSSION

### The overall structure of LZ-8

To perform a comparative structural analysis, we solved the crystal structure of LZ-8 at 2.10  $\text{Å}$  resolution. The crystal belongs to the space group of  $P2_12_12_1$ , with a unit cell of  $a = 33.19 \text{ \AA}$ ,  $b = 86.99 \text{ \AA}$ ,  $c = 92.13 \text{ \AA}$  and  $\alpha = \beta = \gamma = 90^\circ$ . Statistics of data collection and crystallographic analyses are listed in Table I. The overall fold of LZ-8 resembles the structure of Fip-fve from *F. velutipes*, which consists of an N-terminal dimerization domain and a C-terminal FNIII domain. The N-terminal domain is composed of an  $\alpha$ -helix and a  $\beta$ -strand that sustains the dimerization via domain swapping,<sup>18</sup> forming a dumb-bell-shaped dimer.<sup>10</sup> The C-terminal FNIII domain belongs to the immunoglobulin-like  $\beta$ -sandwich fold and comprises a sandwich structure of two  $\beta$ -sheets (I and II) formed by  $\beta$ -strands A-B-E and G-F-C-D, respectively (Fig. 1A). To our knowledge, the crystal structure of LZ-8 is the second structure of fungal immunomodulatory proteins to date.<sup>19</sup>

### Possible structural basis of the LZ-8 antitumor activity

To survey the “hotspots” for the antitumor activity, a structure-based multialignment was performed (Fig. 1B).

**Figure 1**

(A) Cartoon representation of LZ-8 dimer.  $\beta$ -Strands in the FNIII domain are labeled as A–G. (B) Structure-based alignment of LZ-8 against other fungal immunomodulatory proteins (Fips). Alignment was performed using MultAlin (<http://prodes.toulouse.inra.fr/multalin>)<sup>26</sup> and ESPrpt.<sup>27</sup> The secondary structural elements are identified from LZ-8 using ESPrpt and displayed at the top of alignment. The  $\alpha$ -helices,  $\beta$ -sheets, and strict  $\beta$ -turns are denoted  $\alpha$ ,  $\beta$ , and TT, correspondingly. Residues of >70% consensus level are in blue rectangle. Completely conserved residues are indicated with white lettering on a red background. The residues involved in loops FG and DE are indicated by asterisks and dots at the bottom of alignment, respectively. (C) Main chain superposition between LZ-8 monomer (yellow) and Fip-fve (pink). LoopDE and loopFG are highlighted in green rectangles.

In total, we found five variable residues located in loopDE, one residue and two gaps in loopFG. In addition, superposition of the LZ-8 structure onto Fip-fve (PDB entry 1OSY)<sup>10</sup> gives a root-mean-square deviation (rmsd) of 0.96 Å over 112  $C_{\alpha}$  atoms. The majority of

large local conformation changes were found in the loopDE and loopFG as well, both of which are exposed at the surface (Fig. 1C). Compared with that of Fip-fve, loopFG of LZ-8 is shorter and protrudes to the opposite direction. LoopDE changes slightly in  $C_{\alpha}$  positions,

resulting in altered orientations of the side chains in this region.

These loops of FNIII-containing proteins are usually involved in specific recognition of their partners which consist of cell hormones, cell adhesion molecules, cytokine receptors, chaperonins, and carbohydrate binding domains.<sup>20,21</sup> Moreover, the corresponding loops of the antibody variable region have been engineered to improve the binding affinity.<sup>22</sup> Sequence analysis of 17 FNIII domains present in human fibronectins revealed large variations in both FG and BC loops,<sup>23</sup> leading to the multiple activities of fibronectins. Randomizing the sequence or length of the loops DE, FG in human fibronectin 10th type III domain has successfully created novel binding proteins to estrogen receptor  $\alpha$ , TNF- $\alpha$ , and Src SH3 domain.<sup>22,24,25</sup>

In conclusion, the conformations of the loops in the FNIII domain of LZ-8 may be a starting point for elucidating the mechanism of specific residues responsible for the antitumor activity. The comparative structural analysis also provided us some clues to improve the medicinal activity via engineering the variable loops.

## ACKNOWLEDGMENTS

The authors thank Mr. Zhiqiang Zhu and Dr. Jiang Yu at USTC for advice on structure solution.

## REFERENCES

1. Tanaka S, Ko K, Kino K, Tsuchiya K, Yamashita A, Murasugi A, Sakuma S, Tsunoo H. Complete amino acid sequence of an immunomodulatory protein, ling zhi-8 (LZ-8): an immunomodulator from a fungus, *Ganoderma lucidum*, having similarity to immunoglobulin variable regions. *J Biol Chem* 1989;264:16372–16377.
2. Kino K, Yamashita A, Yamaoka K, Watanabe J, Tanaka S, Ko K, Shimizu K, Tsunoo H. Isolation and characterization of a new immunomodulatory protein, ling zhi-8 (LZ-8), from *Ganoderma lucidum*. *J Biol Chem* 1989;264:472–478.
3. Miyasaka N, Inoue H, Totsuka T, Koike R, Kino K, Tsunoo H. An immunomodulatory protein, Ling Zhi-8, facilitates cellular interaction through modulation of adhesion molecules. *Biochem Biophys Res Commun* 1992;186:385–390.
4. van der Hem LG, van der Vliet JA, Kino K, Hoitsma AJ, Tax WJ. Ling-Zhi-8: a fungal protein with immunomodulatory effects. *Transplant Proc* 1996;28:958–959.
5. Murasugi A, Tanaka S, Komiyama N, Iwata N, Kino K, Tsunoo H, Sakuma S. Molecular cloning of a cDNA and a gene encoding an immunomodulatory protein, Ling Zhi-8, from a fungus, *Ganoderma lucidum*. *J Biol Chem* 1991;266:2486–2493.
6. Haak-Frendscho M, Kino K, Sone T, Jardieu P. Ling Zhi-8: a novel T cell mitogen induces cytokine production and upregulation of ICAM-1 expression. *Cell Immunol* 1993;150:101–113.
7. Liao CH, Hsiao YM, Sheu GT, Chang JT, Wang PH, Wu MF, Shieh GJ, Hsu CP, Ko JL. Nuclear translocation of telomerase reverse transcriptase and calcium signaling in repression of telomerase activity in human lung cancer cells by fungal immunomodulatory protein from *Ganoderma tsugae*. *Biochem Pharmacol* 2007;74:1541–1554.
8. Liao CH, Hsiao YM, Hsu CP, Lin MY, Wang JC, Huang YL, Ko JL. Transcriptionally mediated inhibition of telomerase of fungal immunomodulatory protein from *Ganoderma tsugae* in A549 human lung adenocarcinoma cell line. *Mol Carcinog* 2006;45:220–229.
9. Ko JL, Hsu CI, Lin RH, Kao CL, Lin JY. A new fungal immunomodulatory protein, FIP-fve isolated from the edible mushroom, *Flammulina velutipes* and its complete amino acid sequence. *Eur J Biochem* 1995;228:244–249.
10. Paaventhan P, Joseph JS, Seow SV, Vaday S, Robinson H, Chua KY, Kolatkar PR. A 1.7Å structure of Fve, a member of the new fungal immunomodulatory protein family. *J Mol Biol* 2003;332:461–470.
11. Leslie AGW. Recent changes to the MOSFLM package for processing film and image plate data. *Joint CCP4 + ESF-EAMCB. Newsletter Protein Crystallogr* 1992;26.
12. Collaborative Computational Project, Number 4. The CCP4 suite: programs for protein crystallography. *Acta Crystallogr D Biol Crystallogr* 1994;50(Pt 5):760–763.
13. Emsley P, Cowtan K. Coot: model-building tools for molecular graphics. *Acta Crystallogr D Biol Crystallogr* 2004;60(Pt 12 Pt 1): 2126–2132.
14. Painter J, Merritt EA. TLSMD web server for the generation of multi-group TLS models. *J Appl Crystallogr* 2006;39:109–111.
15. Davis IW, Leaver-Fay A, Chen VB, Block JN, Kapral GJ, Wang X, Murray LW, Arendall WB, 3rd, Snoeyink J, Richardson JS, Richardson DC. MolProbity: all-atom contacts and structure validation for proteins and nucleic acids. *Nucleic Acids Res* 2007;35 (Web Server issue):W375–W383.
16. Laskowski RA, MacArthur MW, Moss DS, Thornton JM. Procheck—a program to check the stereochemical quality of protein structures. *J Appl Crystallogr* 1993;26:283–291.
17. DeLano WL. The PyMOL molecular graphics System. San Carlos, CA: DeLano Scientific LLC. Available at: <http://www.pymol.org>.
18. Bennett MJ, Schlunegger MP, Eisenberg D. 3D domain swapping: a mechanism for oligomer assembly. *Protein Sci* 1995;4:2455–2468.
19. Barton GJ. Scop: structural classification of proteins. *Trends Biochem Sci* 1994;19:554–555.
20. Bork P, Doolittle RF. Proposed acquisition of an animal protein domain by bacteria. *Proc Natl Acad Sci USA* 1992;89:8990–8994.
21. Campbell ID, Spitzfaden C. Building proteins with fibronectin type III modules. *Structure* 1994;2:333–337.
22. Koide A, Abbatiello S, Rothgery L, Koide S. Probing protein conformational changes in living cells by using designer binding proteins: application to the estrogen receptor. *Proc Natl Acad Sci USA* 2002;99:1253–1258.
23. Main AL, Harvey TS, Baron M, Boyd J, Campbell ID. The three-dimensional structure of the tenth type III module of fibronectin: an insight into RGD-mediated interactions. *Cell* 1992;71:671–678.
24. Koide A, Bailey CW, Huang X, Koide S. The fibronectin type III domain as a scaffold for novel binding proteins. *J Mol Biol* 1998; 284:1141–1151.
25. Karatan E, Merguerian M, Han Z, Scholle MD, Koide S, Kay BK. Molecular recognition properties of FN3 monobodies that bind the Src SH3 domain. *Chem Biol* 2004;11:835–844.
26. Corpet F. Multiple sequence alignment with hierarchical clustering. *Nucleic Acids Res* 1988;16:10881–10890.
27. Gouet P, Robert X, Courcelle E. ESPript/ENDscript: extracting and rendering sequence and 3D information from atomic structures of proteins. *Nucleic Acids Res* 2003;31:3320–3323.